南京航空航天大學
NANJING UNIVERSITY OF AERONAUTICS AND ASTRONAUTICS

PROCEEDINGS OF

2018 INTERNATIONAL ACADEMIC CONFERENCE FOR GRADUATES NUAA

VOLUME A5

Hosted by
Graduate School, NUAA
College of International Education, NUAA
Association for Science and Technology, NUAA

October 17th-19th, 2018, Nanjing, China

CONTENTS

A Novel Variable Stiffness Continuum Manipulator with a SMA-based Sheath for Minimally Invasive Surgery

Yanfei Cao *, Feng Ju, Bai Chen

* College of Mechanical and Electrical Engineering
Nanjing University of Aeronautics and Astronautics, Nanjing 210016, China
Email: caoyanfei94@163.com

Abstract

This paper proposes a novel variable stiffness continuum manipulator for minimally invasive surgery (MIS). Each module is integrated with a variable stiffness sheath based on shape memory alloy (SMA), which is able to continuously tune stiffness under different voltages, along with the phase transformation of SMA between austenite and martensite. In this paper, the conceptual design, theoretical modeling and finite element method (FEM) simulation are presented. Moreover, the memorized shape setting process of SMA and fabrication of the single module are carried out. Finally, thermo-electric behavior characterization of SMA and stiffness characterizations of the module are separately studied experimentally.

***Keywords*: Continuum manipulator, variable stiffness, shape memory alloy, minimally invasive surgery.**

I. INTRODUCTION

Benefiting from less invasion, less postoperative pain, shorter recovery time and fewer postoperative complications compared with conventional surgery, minimally invasive surgery (MIS) has become the latest trend in surgical field [1]. MIS is usually associated with a limited view of the surgical area and difficult handling of the surgical tools, however, which can be overcome with the assistance of continuum manipulators [2].

In contrast to conventional rigid-link manipulators, continuum manipulators possess their own distinct advantages and characteristics: predominant flexibility, multi degrees of freedom (DOFs), outstanding obstacle avoidance ability and high possibility for miniaturization [3]. And main parts of mechanical structures in continuum manipulators are mostly made of soft materials like silicone or rubber, which contributes to the advantage of high flexibility, as well as several drawbacks like poor rigidity and low load capacity. To be specific, as shown in Fig. 1, during the movement of the continuum manipulator, lacking enough stiffness greatly affects the accuracy of motion, due to the coupling effect among adjacent modules. In addition, a continuum manipulator with high stiffness can tolerate high external force without obvious mechanical deformation while manipulating a heavy surgical tool and interacting with surrounding tissues. Hence, a continuum manipulator with variable stiffness represents a way to safely navigate inside the body, monitoring the interactions with tissues and reducing operational difficulty for surgeon [4].

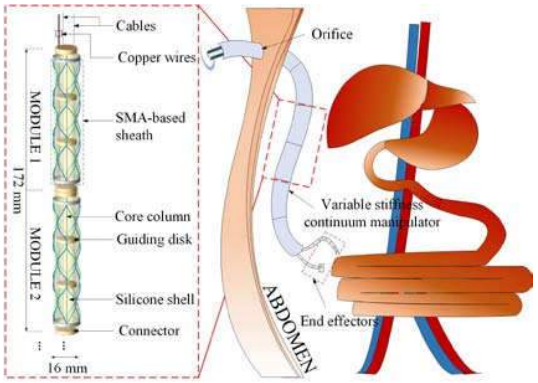

Fig. 1. Envisaged surgical scenario of an abdominal task with a variable stiffness continuum manipulator composed of multiple homogenous modules.

In recent years, more and more researchers have devoted in investigations on variable stiffness of continuum manipulators for MIS. Intelligent materials like magnetorheological (MR) or electrorheological (ER) fluids are focused on due to their variable physical properties [5-6]. Phase change materials, such as paraffin, solder, thermoplastic polymers, low melting point liquid metal (LMPA) and so on, have become a new research hotspot [7-8]. In spite of a wide range of changes in stiffness and strength for phase change materials, most phase change materials have a relatively longer activation timescale compared with others. In addition, granular jamming technology based on granular media has recently been focused on in the field of variable stiffness [9]. Although significant stiffness can be obtained via granular jamming, a substantial volume of grains is required. Besides, layer jamming technology is an emerging method for variable stiffness [10], which depends on controlling the friction between layered structures inside the modules of the manipulator. And it is relatively difficult for application on medical flexible manipulators.

In this paper, the authors present a novel approach to variable stiffness for continuum manipulators, referring to a

SMA-based variable stiffness sheath integrated in each module actuated by applied voltages, as shown in Fig. 1. SMA is well suited for MIS applications due to excellent properties of low driving voltage, suitable phase transformation temperature, easy miniaturization and crucial biocompatibility, etc. And this approach to variable stiffness has comparable stiffness tuning performance due to fast transformation rate, compact size, and obvious stiffness range. All the components of the single module in the proposed variable stiffness flexible manipulator are detailed in terms of the design, modeling, simulations, fabrication, and experimental characterizations for variable stiffness performance.

II. Conceptual Design Of The Manipulator

A. Configuration and principle

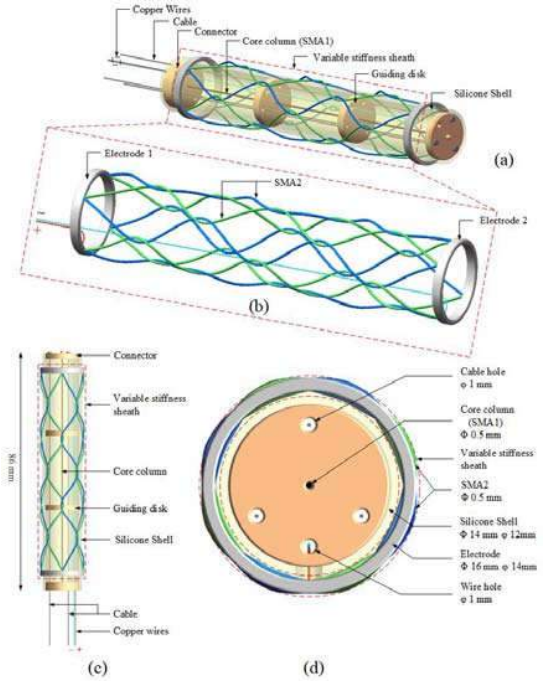

Fig. 2. Single module design from different views. (a) Axonometric view. (b) Magnified view of the variable stiffness sheath. (c) Longitudinal view. (d) Cross-section view. In the cross-section view, the dimensions of relevant parts are marked, and the variable stiffness sheath is highlighted with a dashed box.

TABLE I
PARAMETERS OF MATERIALS USED IN THE MANIPULATOR

Material	Parameter	Value
SMA-1	Diameter	0.5 mm
	Length	83 mm
	Elastic modulus	55 GPa
SMA-2	Diameter	0.5 mm
	Length	72 mm
	Poisson's ratio	0.33
	Density	5000 kg/m^3
	Austenite start temperature	28 ℃
	Austenite finish temperature	49 ℃
	Martensite start temperature	41 ℃
	Martensite finish temperature	26 ℃
	Martensite elastic modulus	26 GPa
	Austenite elastic modulus	67 GPa
	Resistance	18 Ω
	Specific heat capacity	1200 J/(kg·℃)
	Heat convection coefficient	1.2 W/(m^2·℃)
	Ambient temperature	25 ℃
Aluminum alloy	Density	2770 kg/m^3
	Elastic modulus	71 GPa
	Poisson's ratio	0.33
ABS plastic	Density	1040 kg/m3
	Elastic modulus	2.37 GPa
	Poisson's ratio	0.43

The designed continuum manipulator is made up of homogenous modular structures (Module 1, 2, …), as shown in Fig. 1. Exactly due to the modular design, the proposed continuum manipulator is suitable for various surgical tasks. Fig.2 shows the configuration of the designed single module from three different views. The main support part of the module is a SMA core column (SMA-1) with superelasticity at room temperature, which ensures the bending motion curve approximated as a constant curvature arc. Two connectors are attached to both ends of the core column, and two guiding disks are distributed along the core column between the connectors. A silicone shell outside these connectors and guiding disks forms a closed cavity for the module. For driving the module to bend in all directions, three flexible cables, 120 degrees apart from each other, are fixed onto the front connector and go through cable holes uniformly distributed at the edge of these guiding disks and connectors.

In particular, a SMA-based variable stiffness sheath, actuated by heating eight wavy SMA wires (SMA-2) woven together, has been integrated into the single module outside the silicone shell. Induced by different temperature stimuli, SMA transforms between two phases separately referred as austenite and martensite, which have completely different crystal structures and material properties. Thus, during the heating process, SMA of the sheath transforms from martensite phase (low elastic modulus) into austenite phase (higher elastic modulus), along with the increase in stiffness of the sheath, and vice versa. However, due to the inherent hysteresis of SMA during phase transformations, stiffness tuning of the sheath shows a certain hysteresis between the heating and cooling processes.

B. Elastic modulus model and thermo-electric model of SMA

SMA, as a family of smart materials, possesses inherent and unique characteristics of superelasticity and shape memory effect. For researching the elastic modulus variation of SMA wires (SMA-2) and validating the variable stiffness performance of the manipulator, the elastic modulus model and the thermos-electric model of SMA are derived. And parameters of SMA involved in derivation are listed in Table 1.

The martensite fraction $\xi(T,\sigma)$ is a crucial parameter to

describe and model phase transformations of SMA [11], which is determined by temperature of SMA T and stress σ. Due to the hysteresis behavior of SMA, two different expressions are given to separately model the variations of $\xi(T,\sigma)$ during the heating and cooling processes of SMA.

During the heating process, SMA gradually transforms from martensite phase into austenite phase. For $A_s+\frac{\sigma}{C_A}\le T\le A_f+\frac{\sigma}{C_A}$, $\xi(T,\sigma)$ is evaluated as

$$\xi(T,\sigma)=\frac{\xi_M}{2}\cos[a_A(T-A_s)+b_A\sigma]+\frac{\xi_M}{2} \tag{1}$$

On the contrary, during the cooling process, SMA gradually transforms from austenite phase into martensite phase. And for $M_f+\frac{\sigma}{C_M}\le T\le M_s+\frac{\sigma}{C_M}$, $\xi(T,\sigma)$ is evaluated as

$$\xi(T,\sigma)=\frac{1-\xi_A}{2}\cos[a_M(T-M_f)+b_M\sigma]+\frac{1+\xi_A}{2} \tag{2}$$

where A_s, A_f, M_s, M_f are separately the start and finish phase transformation temperatures of austenite and martensite phases. ξ_M, ξ_A are separately the initial martensite fraction of the mentioned two processes. And $\xi_M=1, \xi_A=0$ is due to that transformations of martensite or austenite are fully completed at the beginning of heating or cooling processes. a_A, b_A, a_M, b_M are constants involved in above four temperatures, which are evaluated as

$$a_A=\frac{\pi}{A_f-A_s}, b_A=-\frac{a_A}{C_A}, a_M=\frac{\pi}{M_s-M_f}, b_M=-\frac{a_M}{C_M} \tag{3}$$

where C_A, C_M are coefficients relevant to stress effects on phase transition temperatures.

Naturally, the elastic modulus model of SMA is given as

$$E(\xi(T,\sigma))=E_A+(E_M-E_A)\xi(T,\sigma) \tag{4}$$

where E_A, E_M are separately elastic modulus values of austenite and martensite phases. Eq. (4) shows that elastic modulus of SMA is relevant to temperature of SMA T and stress σ. It is assumed that no stress is applied to SMA wires in the proposed variable stiffness sheath, and thus $\sigma=0$. However, it is practically difficult to accurately measure temperature of SMA wires due to its small dimension and disturbance of ambient conditions. Consequently, a thermo-electric model is essential for modelling SMA wire temperature T under different voltage stimuli.

The simplified thermo-electric model that describes the temperature variation of SMA under voltage stimuli and ambient temperature condition [12] is given as

$$\rho v c_P\frac{\mathrm{d}T(t)}{\mathrm{d}t}=\frac{U^2}{R_{SMA}}-h_cA_c[T(t)-T_a] \tag{5}$$

where $v=\frac{\pi d^2 l}{4}$ is the volume of SMA wires. ρ, d, l, c_P are separately the density, diameter, length and specific heat capacity of the wire. U is the voltage between both ends of SMA wires. R_{SMA} is the resistance of SMA wires, which is assumed to be a constant. h_c is the convective heat transfer coefficient. $A_c=\rho dl$ is the convective surface area of the wire. T_a is the ambient temperature. Then, via integration of Eq. 5, the SMA wire temperature T is given as

$$T-T_a=(T_0-T_a)\mathrm{e}^{-\frac{t}{\tau}}+\frac{U^2}{h_cA_cR_{SMA}}(1-\mathrm{e}^{-\frac{t}{\tau}}) \tag{6}$$

where T_0 is the initial temperature of SMA wires. $\tau=\frac{\rho v c_P}{h_cA_c}$ is the time constant. Considering $T_0=T_a$, Eq. 6 is rewritten as

$$T=T_a+\frac{U^2}{h_cA_cR_{SMA}}(1-e^{-\frac{t}{\tau}}) \tag{7}$$

From Eq. (7), the parameters needed to be measured for obtaining the temperature of SMA T is potential difference U and related constants listed in Table 1.

C. FEM simulation for variable stiffness

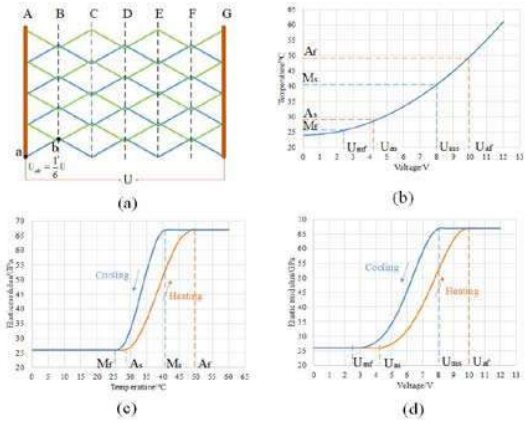

Fig. 3. Thermo-electric behavior simulation of the SMA-based sheath. (a) Circuit analysis of the sheath when voltage U is applied between two electrodes. (b) Temperature-voltage simulation curve of SMA. (c) Elastic modulus-temperature simulation curve of SMA. (d) Elastic modulus-voltage simulation curve of SMA. And eight essential temperature parameters and voltage parameters (As, Af, Ms, Mf, Uas, Uaf, Ums, Amf) are shown in (b)-(d).

This section is devoted to accomplishing the FEM simulation for variable stiffness. Before FEM simulations, aimed at the proposed configuration of the SMA-based sheath, the relationship between elastic modulus of SMA and voltage applied on the entire sheath needs discussions. Due to the

interconnections of SMA wires, each SMA wire can be divided into six segments (segment ab is one among them) at the bending corners from left to right, forming six relatively independent areas named AB to FG (A to F are separately equipotential surfaces), as shown in Fig. 3. (a). Each segment in an area is connected in parallel with other segments in the same area, and segments in adjacent areas are connected in series. Assuming that each segment has the same dimension in diameter and length, equal amount of voltage is distributed to each segment like segment ab, $U_{ab} = \frac{1}{6}U$ (i.e., these SMA segments are under the same heating or cooling condition). Based on Eq. (1), (2), (4) and (7), Fig. 3. (b), (c) and (d) separately show temperature-voltage, elastic modulus-temperature and elastic modulus-voltage simulation curves of SMA segments. When voltage U ranges from U_{as} to U_{af}, SMA temperature rises from A_s to A_f, along with phase transforms from martensite into austenite. On the contrary, when voltage U ranges from U_{ms} to U_{mf}, SMA temperature rises from M_s to M_f, along with phase transforms from austenite into martensite. And the hysteresis of elastic modulus is distinct during the cooling process.

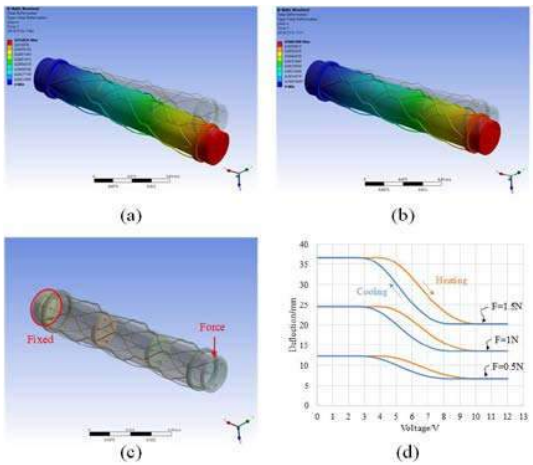

Fig. 4. Results of FEM simulation for the single module integrated with the variable stiffness sheath via static structural analysis. (a) Deformation nephogram of the module, in an unactuated state (flexible state) and under 0.5 N force. (b) Deformation nephogram of the module, in a fully actuated state (rigid state) and under 0.5 N force. (c) Three-dimensional models and corresponding boundary conditions of the module. (d) Deflection-voltage simulation curves of the module during heating and cooling processes, separately under forces of 0.5 N, 1 N, 1.5 N.

In FEM simulations, the static structural analysis for the single module integrated with the SMA-based sheath is performed. Three-dimensional models of the module and boundary conditions are shown in Fig. 4. (c). Relevant parameters of materials set in the simulations are listed in Table 1. In addition, corresponding elastic modulus values of SMA under different voltages during heating and cooling processes are obtained from simulation results in Fig. 3. (d). Fig. 4. (a) and (b) show deformation nephograms of the module under 0.5 N force, separately in an unactuated state (flexible state) and a fully actuated state (rigid state). And deflection-voltage simulation curves of the module are shown in Fig. 4. (d). It is clearly seen that when voltage increases from 0 to 10 V, the deflection reaches to the minimum during the heating process, meaning that stiffness of the module reaches to the maximum. The maximum $D_{\max}$ and minimum $D_{\min}$ of the deflection for force 0.5 N, 1 N and 1.5 N are separately 12.2352 mm and 6.7408 mm, 24.4704 mm and 13.4816 mm, 36.7056 mm and 20.2224 mm. And the increment of stiffness $D_{\max} / D_{\min} - 1$ is 81.5%.

III. Module Fabrication

A. Memorized shape setting process of SMA

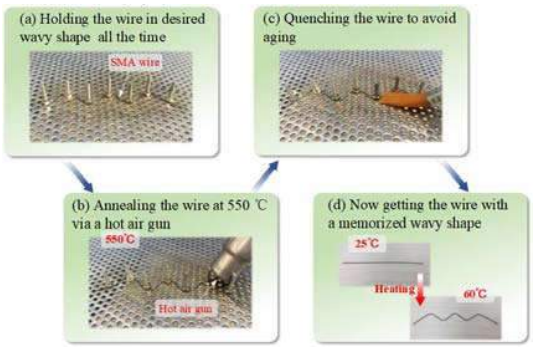

Fig. 5. Manual operation steps for memorized shape setting process of SMA wires.

For fabricating the proposed SMA-based variable stiffness sheath by weaving wavy SMA wires together, it is extremely essential to carry out memorized shape setting process for SMA wires. In this case, the sheath can hold its initial shape (i.e., all the woven SMA wires hold their wavy memorized shape) during the stiffness-tuning process.

As shown in Fig. 5, the memorized shape setting process for selected SMA wires is manually performed after several steps. First, a stainless-steel sieve plate with numerous 2-mm-diameter holes distributed equidistantly on the surface, eight SMA wires, seven groups of screws and nuts with a 1.6 mm diameter are prepared. The wire is folded in a wavy shape and then fixed on the surface of the sieve plate via screws and nuts, as shown in Fig. 5. (a). For setting the memorized shape, the wire is then annealed at a temperature around 550 ℃ via a hot air gun, as shown in Fig. 5. (b). Here, the appropriate annealing time is about 30 seconds, which depends on wire diameter. After that, the desired wavy memorized shape of the SMA wire is obtained. Last but not least, the wire is quenched to avoid aging, as shown in Fig. 5. (c).

The verification for the memorized shape setting process is then performed. As shown in Fig. 5. (d), left, the processed

wire is straightened manually at the room temperature around 25 ℃. Once heated around 60 ℃ just above A_f, the shape of the processed wire transforms into its new memorized shape of a wavy line due to the phase transformation of SMA from martensite into austenite, along with the increase in elastic modulus as shown in Fig. 5. (d), right. And during the cooling process, the wire still holds the wavy memorized shape under no external stress, but the phase of SMA gradually transforms from austenite into martensite, along with the decrease in elastic modulus.

B. Fabrication of the single module

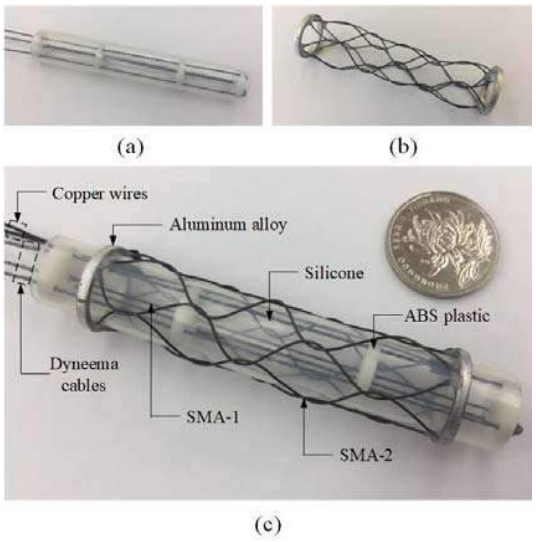

Fig. 6. Fabrication of the variable stiffness continuum manipulator. (a) The continuum structure without the variable stiffness sheath. (b) The SMA-based variable stiffness sheath. (c) The single module integrated with the sheath. And relevant materials used in the fabrication are shown.

Components of the single module of the continuum manipulator are a continuum structure and a SMA-based variable stiffness sheath. The continuum structure is composed of a silicone shell with a 12mm-diameter lumen, a SMA core column (SMA-1), four ABS plastic connectors and guiding disks, three circumferentially distributed dyneema cables and two copper wires, as shown in Fig. 6. (a). And the SMA-based variable stiffness sheath is woven by eight SMA wires (SMA-2), which have a memorized shape of a wavy line, as shown in Fig. 6. (b). Then, the single module of the variable stiffness continuum manipulator is obtained by integrating the sheath with the continuum structure, as shown in Fig. 6. (c).

IV. Experimental Characterization

A. Thermo-electric behavior of the SMA

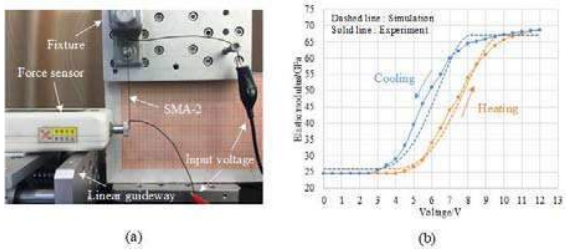

Fig. 7. Experimental characterization for thermo-electric behavior of SMA. (a) Setup for experimental measurement of relationships between elastic modulus and voltage. (b) Elastic modulus-voltage experimental curve of SMA.

In order to verify the relationship between the elastic modulus and voltage of SMA wire obtained from theoretical models (Eq. (4) and (7)), the thermo-electric behavior of the SMA wire is experimentally characterized.

The setup for this experimental characterization is shown in Fig. 7. (a). A SMA wire (SMA-2) with a 0.5 mm diameter and 10 mm length is selected for this characterization. One end of the wire is fixed to a fixture, and the opposite end is in its free state vertically. The wire is heated by applying a controllable voltage, ranging from 0 to 12 V, between two ends of the wire. The elastic modulus of SMA under different voltages is distinctly different, which can be obtained by means of the cantilever beam model given as

$$E = \frac{FL^3}{3I\delta} \tag{8}$$

Where E is the elastic modulus of SMA to be obtained. F is the force imposed at the free end of the wire via a digital force sensor (SH-5, SUNDOO, Japan, resolution = 0.001 N, measuring range = 5 N) fixed on a linear guideway horizontally. L is the wire length. $I = \frac{\pi d^4}{64}$ is the inertia moment constant of the wire relevant to the diameter of wire d. And δ is the deflection of the free end to be measured. Fig. 7. (b) shows the elastic modulus-voltage experimental curve of the SMA wire. And the elastic modulus at each point of voltage ranging from 0 to 12 V with an interval of 0.5 V is repeatedly measured three times. As it can be seen, the minimum and maximum of the elastic modulus are separately 24.5 GPa and 68.6 GPa during the heating and cooling processes from experimental data. And the experimental results (Solid lines) are in qualitative agreement with the simulation curves (dashed lines) based on theoretical models.

B. Variable stiffness characterization of the single module

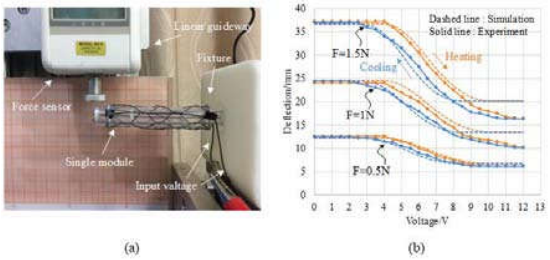

Fig. 8. Stiffness characterizations of the single module integrated with the sheath. (a) Setup for variable stiffness test of the module. (b) Deflection-voltage experimental curves of the module during heating and cooling processes, separately under forces of 0.5 N, 1 N, 1.5 N.

The variable stiffness performance of the single module is experimentally characterized, as is shown in Fig. 8. (a). In the setup, one end of the module is fixed and a controllable force is imposed at the other free end via the digital force sensor fixed on a linear guideway vertically. A controllable voltage, ranging from 0 to 12 V with an interval of 0.5 V, is applied between both ends. Fig. 8. (b) shows comparisons between simulation and experimental results of deflection-voltage curves under different forces of 0.5 N, 1 N and 1.5 N, separately during the heating and cooling processes. As expect, it can be clearly seen that deflection of the free end gradually decreases (i.e., stiffness of the module increases) under three load situations in the heating process. And the decrease of stiffness in the cooling progress is distinctly lag behind the increase of stiffness in the heating process, which shows qualitative agreement with the simulation data. Differential parts between experimental results and simulation ones could derive from simplifications made in model and inherent errors of the measuring system. In general, the maximum $D_{\max}$ and minimum $D_{\min}$ among deflections for force 0.5 N, 1 N and 1.5 N are separately 12.6 mm and 6.2 mm, 24.4 mm and 10.2 mm, 37.2 mm and 16.4 mm. And the increments of stiffness are separately 103.2%, 139.2%, 126.8%.

V. Conclusion

This paper introduces a novel continuum manipulator with a SMA-based variable stiffness sheath for MIS. And the stiffness of the sheath can be adjusted continuously as a voltage between both ends of the sheath ranges in a reasonable range, along with the phase transformations between austenite and martensite. Precisely due to this, the accuracy, safety and stability for continuum manipulators during MIS can increase potentially. In detail, the design, modeling, FEM simulations, fabrication and experimental characterizations for the proposed sheath and single model are separately presented. As expected, experimental results demonstrate that the stiffness of the single module are able to increase up to 139.2 %, which show qualitative agreement with simulation ones.

For future research, the improvement for variable stiffness capacity of the continuum manipulator by means of structure optimization and material selections will be considered. Furthermore, miniaturization possibilities aimed at enhancing suitability for medical applications in MIS will be focused on.

Acknowledgement

This work is supported by the National Natural Science Foundation of China (No.51575256, No.51705243).

References

[1] V. Vitiello, S. Lee, T. Cundy, G. Yang. Emerging Robotic Platforms for Minimally Invasive Surgery. *IEEE Reviews in Biomedical Engineering,* vol.6, pp.111-126, 2013.

[2] Jones Bryan A, Walker Ian D. Kinematics for multisection continuum robots. *IEEE Trans Rob* 2006;22(1):43–55.

[3] S. Shaikh and C. Thompson. Natural orifice translumenal surgery: Flexible platform review. *World J. Gastrointestinal Surg.*, vol. 2, no. 6, pp. 210–216, Jun. 2010.

[4] M. Mahvash, P. E. Dupont. Stiffness Control of Surgical Continuum Manipulators. *IEEE Transactions on Robotics*, vol. 27, no. 2, pp. 334-345, 2011.

[5] G. Olson. Medical devices with variable stiffness. ed: Google Patents, 2013.

[6] Alex S. Shafer and Mehrdad R. Kermani. On the Feasibility and Suitability of MR Fluid Clutches in Human-Friendly Manipulators. IEEE Transactions on Mechatronics, vol. 16, no. 6, pp. 1073-1082, 2011.

[7] F. Alambeigi, R. Seifabadi, and M. Armand. A continuum manipulator with phase changing alloy. in 2016 IEEE International Conference on Robotics and Automation (ICRA), 2016, pp. 758-764.

[8] Huu Minh Le, Thanh Nho Do, Lin Cao and Soo Jay Phee. Towards Active Variable Stiffness Manipulators for Surgical Robots. *2017 IEEE International Conference on Robotics and Automation*, 2017, pp. 1766-1771.

[9] Tommaso Ranzani, Matteo Cianchetti. A Soft Modular Manipulator for Minimally Invasive Surgery- Design and Characteri-zation of a Single Module. *IEEE Transactions on Robotics*, 32(1): 187-200, 2016.

[10] Jessie Lee C. Santiago, Isuru S. Godage, Phanideep Gonthina, and Ian D. Walker. Soft Robots and Kangaroo Tails: Modulating Compliance in Continuum Structures Through Mechanical Layer Jamming. *Soft Robotics,* vol. 3, no. 2, pp. 54-63, 2016.

[11] Dutta S M, Ghorbel F H. Differential hysteresis modeling of a shape memory alloy wire actuator. *IEEE/ASME Transactions on Mechatronics*, 10(2):189-197, 2005.

[12] Meier H, Oelschlaeger L. Numerical thermomechanical modelling of shape memory alloy wires[J]. *Materials Science & Engineering A*, 2004, 378(1–2):484-489.